arXiv:1512.01478v1 [cs.NI] 4 Dec 2015

A Stochastic Geometry Framework for Asynchronous Full-Duplex Networks

Andrea Munari, *Member IEEE*, Petri Mähönen, *Senior Member IEEE*,
Marina Petrova, *Senior Member IEEE*

Institute for Networked Systems, RWTH Aachen University, Kackertstrasse 9, 52072 Aachen, Germany

e-mail: {andrea.munari, petri.mahonen, marina.petrova}@inets.rwth-aachen.de.

Abstract

In-band full-duplex is emerging as a promising solution to enhance throughput in wireless networks. Allowing nodes to simultaneously send and receive data over the same bandwidth can potentially double the system capacity, and a good degree of maturity has been reached in terms of physical layer design with practical demonstrations in simple topologies. However, the true potential of full-duplex at a system level is yet to be fully understood. In this paper, we introduce an analytical framework based on stochastic geometry that captures the behaviour of large full-duplex networks implementing an asynchronous random access policy. Via closed-form expressions we discuss the key tradeoffs that characterise these systems, exploring among the rest the role of transmission duration, imperfect self-interference cancellation and fraction of full-duplex nodes in the network. We also provide protocol design principles, and our comparison with slotted systems sheds light on the performance loss induced by the lack of synchronism.

Index Terms

Full-Duplex, Stochastic Geometry, Random Access.

The material in this paper was presented in part at the EAI International Conference on Future Access Enablers of Ubiquitous and Intelligent Infrastructures 2015.

I. Introduction

The inability for a radio to send and receive information at the same time over the same frequency band has represented for decades a cornerstone in the design of wireless communications systems. Such a constraint stems from the simple observation that the power radiated by a terminal impinges on its own receive antenna with low – if any – attenuation, inducing an additional noise that easily disrupts retrieval of incoming packets. Despite conceptually simple, in fact, the task of effectively cancelling a known transmitted message from a received waveform has long remained elusive for practical real-time implementations given the unbalance of several orders of magnitude between the desired signal and the superposed self-generated interference.

This classical state of the art has witnessed a tremendous change of perspective in the past few years. Indeed, the compelling quest for higher throughput and spectral efficiency, coupled with steady advances in signal processing and computational processing power has driven a lot of research attention to the careful design of advanced self-interference suppression schemes. This has eventually made the in-band full-duplex concept practical [1], [2]. Following the path outlined by these seminal works, several approaches were later proposed to prove the viability of simultaneous transmission and reception over the same bandwidth for devices in ad-hoc and cellular networks (see, e.g., [3]–[6], [7], [8] and references therein). Typically, full-duplex radios resort to three stages for handling interference: *passive* attenuation (carefully separating transmit and receive antennas to induce a higher path-loss), *analog* suppression (leaning on circuitry to subtract a weighed version of the own signal from the incoming waveform); and *digital* cancellation (resorting to signal processing algorithms). Remarkably, most such solutions have been validated via software defined radios or through prototypes employing off-the-shelf hardware, buttressing a future implementation of the full-duplex principle onto low-cost terminals. With this horizon in mind, and allured by a potential throughput doubling, a number of protocols at the medium access layer have been designed [5], [9]–[12], showing by means of simulations and testbed results interesting improvements over a half-duplex configuration in centralised as well as in distributed ad-hoc scenarios based on the IEEE 802.11 standard. Alongside with these efforts, information theoretic tools helped in clarifying the potential of concurrent transmission and reception in toy topologies, exploring the achievable rate regions and the degrees of freedom for such technology in relation to the accuracy in self-interference cancellation and the number

of available antennas [13]–[17].

Despite having reached a reasonable maturity in the physical layer design of a single link, a deep understanding of the role played by full-duplex at a network level is still elusive. In fact, when instantiated in broad topologies, the novel paradigm triggers a non-trivial tradeoff between spatial reuse and aggregate interference. On the one hand, the ability to leverage simultaneous bidirectional data exchanges within node pairs allows more links to be active per unit area, potentially boosting performance. On the other hand, the additional amount of interference generated by a more aggressive access to the medium besets ongoing receptions, decreasing the probability of successfully retrieving information. The overall balance of such counterposed effects on throughput as well as the influence of more articulated traffic patterns on full-duplex connections are only a few of the open questions that still need to be carefully addressed. Particularly, a clear theoretical perspective to derive some general design principles for next-generation wireless networks is yet to be grasped. Some relevant steps in this direction were taken in [18], [19] following different approaches. In the first contribution, the authors focused on the well-known protocol model introduced by Gupta and Kumar [20]. Assuming that power only propagates within a circle area centred at the transmitter, they evaluated the throughput gain over half-duplex in linear and lattice topologies with centrally scheduled communications, and proved that the harsher interference level brought by full-duplex intrinsically prevents a network-wide throughput doubling. This trend was buttressed by Haenggi et al. in [19], which, leaning on stochastic geometry, broadened its applicability to a more realistic interference model and to a completely decentralised medium access based on slotted Aloha, offering an elegant characterisation of the performance dependence on several system design parameters.

While very insightful, these results are derived considering *perfect* synchronisation among all nodes. On the other hand, the potential of full-duplex within the complementary and broad family of asynchronous systems is yet to be explored. From this viewpoint, for instance, the novel paradigm is gaining attention for cognitive scenarios – where terminals not even sharing a common access protocol contend for the medium [21], and is regarded as a key concept for next generation ad hoc networks and machine type communications (MTC) in 5G systems [22] to tackle a massive number of wireless devices that exchange information in a fully decentralised and sporadic fashion. For such applications, maintaining a common time reference may either be unfeasible or simply not worth due to complexity and cost, prompting asynchronous random

access as the natural choice. Moreover, data exchanges of different duration are likely to populate the channel, with long and periodic packet transmissions flanked by bursty short information units typical of MTC, inducing a highly time-varying interference.

Understanding whether full-duplex capabilities can be effectively leveraged in scenarios facing such challenges is thus paramount for proper system design, and represents a deciding element towards identifying applications that can truly benefit from the new paradigm. In this paper we tackle this fundamental and still open question, introducing tools to evaluate the performance of a full-duplex implementation in large, uncoordinated and asynchronous networks as a function of the traffic profile to be served, the self-interference cancellation capabilities and other relevant parameters. Within this paper, we provide the following main contributions:

- Introducing an analytical framework based on stochastic geometry, we characterise the performance of an asynchronous Aloha system where a fraction of nodes are capable to operate in full-duplex. Closed form expressions for the success probability at a link level as well as for the aggregate network throughput are derived, accounting for residual self-interference that besets full-duplex nodes and insightfully isolating and discussing the impact of design parameters such as transmission duration and distance between transmitter and receiver.
- Assuming all links to be of the same duration, we identify different optimal operating regions for the system. In particular, we show how full-duplex shall be preferred for short packet exchanges, whereas for transmissions longer than a specified threshold the whole network shall be operated in half-duplex to avoid throughput losses.
- We explore the additional degree of freedom of having transmissions of different duration in the network and derive the optimal working configuration in this case, significantly extending the applicability of the analytical framework
- We finally offer a comparison with the results derived in [19] for a slotted medium access, and discuss the throughput degradation induced by the lack of synchronisation among nodes as a function of the fraction of full-duplex links active in the network, offering a tool to approach a key cost-performance tradeoff in system planning.

We start our study in Section II introducing the system model and some preliminary results on stochastic geometry, later leveraged in Section III to derive the performance of an asynchronous

full-duplex network. Sections IV and V extend the framework to account for different packet durations and offer a comparison with slotted schemes, eventually leading to the conclusions drawn in Section VI.

II. System Model and Preliminaries

Throughout this paper we focus on an infinite population of users spread over the plane that share a common medium to exchange information in the form of data packets. Nodes are organised in pairs or *clusters*, and only one-hop links between a terminal and its pair-companion are considered. We indicate the two users within cluster $\mathcal{C}_i$ as U_i and V_i, and specify their location by means of the two-dimensional coordinate vectors $\mathbf{u}_i$ and $\mathbf{v}_i$, respectively. Without loss of generality, we assume each pair in the network to be separated by a common distance $r \geq 1$, i.e., $\|\mathbf{u}_i - \mathbf{v}_i\| = r, \ \forall i$.[1]

Clusters can be operated either in *half-duplex* or *full-duplex* mode. In the former case, one terminal transmits packets according to the underlying medium access strategy, while the other simply acts as receiver and does not generate any traffic. As to the latter mode, instead, both nodes in the pair access the channel simultaneously, leveraging in-band full-duplex capabilities to send and receive data at the same time over the same frequency. In order to cover a broad range of configurations, we assume that a fraction q of clusters resort to full-duplex operations, whereas the remaining perform half-duplex access.

Communication parameters in terms of bitrate, modulation and coding are, unless otherwise specified, common to all terminals and set for every transmission to last D seconds. Medium contention is performed asynchronously via random access, following a simple unslotted Aloha protocol, and no feedback nor retransmission policy are considered. Following this approach, transmissions are performed without sensing the surrounding activity and without adhering to any slotted time structure. The only form of coordination we consider in the network is thus between users of the same pair, assuming the receiver to be always listening to the incoming transmission of its companion in a half-duplex cluster, or both nodes to simultaneously start a reciprocal transmission in the full-duplex configuration. In this perspective, while we abstract here any

[1]While the results presented in this paper can easily be extended to an arbitrary distribution for the pair distance, the hypothesis of a common value for r allows to ease the mathematical discussion while prompting all the key tradeoffs in the system.

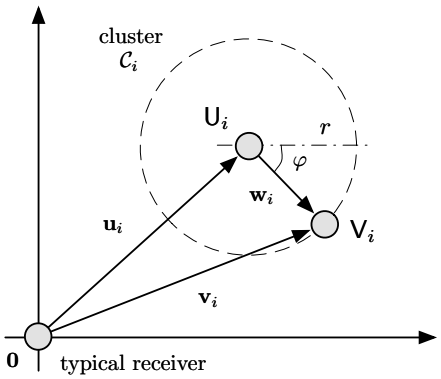

Fig. 1: Reference geometry for the links between a typical receiver located at the origin and nodes within cluster $\mathcal{C}_i$.

further details for the sake of generality and mathematical tractability, it is worth mentioning that different strategies have been proposed in the literature to bring such coordination into practice, see, e.g., [5], [11], [12].

In order to capture the behaviour of such a system, we introduce an analytical framework based on stochastic geometry, and model links in the network via a homogeneous time-space Poisson point process (PPP) $\Lambda = \{\mathbf{u}_i, T_i\}$ of intensity λ. With reference to the topology of Fig. 1, the spatial component $\mathbf{u}_i$ of the process describes the location of terminal U_i, also referred to as the *cluster center*, which, in case of a half-duplex pair, acts as transmitter. The companion node V_i is instead randomly scattered over a circle of radius r centred at U_i, allowing its position to be expressed as $\mathbf{v}_i = \mathbf{u}_i + \mathbf{w}_i$, where $\mathbf{w}_i = re^{j\varphi_i}$ and $\varphi_i \sim \mathcal{U}(0, 2\pi)$. In turn, the temporal component T_i of Λ identifies the start time of the transmission performed by cluster $\mathcal{C}_i$. From this standpoint, it is important to stress that we do not focus on a spatial point process describing the distribution of nodes and track the evolution of their unslotted medium access over time, e.g., by resorting to a renewal process. Conversely, Λ jointly captures position and transmission time of a cluster, modelling the network as a population of node pairs that are born at a random time and a random location and occupy the channel for a predefined time D before disappearing. This approach introduces a further level of abstraction, as it embeds in the sole parameter λ the spatial density of the population and the traffic generation pattern, as well as possible backoff strategies applied to the medium access contention. On the other hand, these working hypotheses

will yield a compact mathematical formulation capable of identifying the key tradeoffs of full-duplex networks, and have been shown to offer a very accurate estimation of the performance of unslotted systems [23]. Moreover, from a practical angle not only can the space-time process under consideration easily be mapped to mobile topologies, but also to scenarios with very large populations of terminals generating sporadic traffic, covering a case of strong interest for MTC applications.

Within this framework, Λ characterises the number N of links established in a region of area A over T seconds, which is described as a Poisson r.v. of parameter λAT:

$$\Pr\{N = n\} = \frac{(\lambda AT)^n e^{-\lambda AT}}{n!}$$

Moreover, the hybrid nature of clusters in the network is accounted for by having each pair independently decide whether to establish a half- or a full-duplex connection with probability $1-q$ and q, respectively. By virtue of the properties of thinning for PPPs (see, e.g., [24]), the original process can then be conveniently expressed as $\Lambda = \Lambda_{\mathsf{hd}} \cup \Lambda_{\mathsf{fd}}$, where Λ_{hd} and Λ_{fd} are two independent PPPs of intensity $(1-q)\lambda$ and $q\lambda$.

Wireless links are affected by path loss and Rayleigh fading, and the coherence time of the wireless channel is assumed long enough for fading coefficients to remain constant throughout the duration of a packet exchange. Accordingly, we model the power received by a node at position $\mathbf{y}$ from a transmission originated at location $\mathbf{x}$ as $P\,L(\mathbf{x},\mathbf{y})\zeta$. Here, P is the transmission power common to all users, ζ is an exponential random variable with unit mean and pdf $f_\zeta(a) = e^{-a}, a \geq 0$ describing fading, and $L(\mathbf{x},\mathbf{y})$ accounts for the signal attenuation. With the aim of focusing on the key performance drivers, we do not explicitly address antenna gains or other propagation factors, and consider instead a simple path-loss law based on the distance $d = \|\mathbf{x}-\mathbf{y}\|$, in the form $L(d) = d^{-\alpha}$, $\alpha > 2$.[2]

The effectiveness of the presented system clearly lives on the tradeoff between the spatial reuse enabled by random access and the mutual interference that besets concurrent links. From this standpoint, it is relevant to stress that the asynchronous nature of the MAC layer under consideration can induce an interference level that is not constant even within the duration of a

[2]Although rigorously the considered path-loss law is only meaningful for $d \geq 1$, extensive results have shown its capability of properly capturing the behaviour of large networks [24]. Moreover, as discussed, we always assume a distance $r \geq 1$ between source and destination within a cluster.

packet exchange. Starting from this remark, and leveraging the homogeneity of the PPP Λ, we focus without loss of generality on a *typical receiver*, i.e., a node at the origin of the plane whose incoming data unit starts at time 0, and derive the time-varying interference $I_{\mathbf{0}}(t)$ it perceives at a generic instant $t \in [0, D]$. To this aim, it is useful to resort to the indicator function $\mathbb{1}(\cdot)$ and introduce the ancillary operator $\iota_i(t) = \mathbb{1}(T_i \leq t \leq T_i + D)$, specifying whether cluster $\mathcal{C}_i$ is active at time t. Moreover, we simplify without risk of confusion the notation for the path-loss, setting for an arbitrary point $\mathbf{x}$ on the plane $L(\mathbf{x}) \triangleq L(\mathbf{x}, \mathbf{0})$. Leaning on these steps, it is possible to isolate the interference contributions $I_{\mathsf{hd}}(t)$ and $I_{\mathsf{fd}}(t)$ of half- and full-duplex pairs, with the former having only one terminal sending data, while the latter triggering two spatially disjoint transmissions. The time-varying interference perceived at the typical receiver can thus be expressed in the form $I_{\mathbf{0}}(t) = I_{\mathsf{hd}}(t) + I_{\mathsf{fd}}(t)$, where

$$\begin{aligned} I_{\mathsf{hd}}(t) &= \sum_{(\mathbf{u}_i, T_i) \in \Lambda_{\mathsf{hd}}} \iota_i(t) \cdot P\, L(\mathbf{u}_i)\, \zeta_i \\ I_{\mathsf{fd}}(t) &= \sum_{(\mathbf{u}_j, T_j) \in \Lambda_{\mathsf{fd}}} \iota_j(t) \cdot P \left(L(\mathbf{u}_j)\, \zeta_j + L(\mathbf{v}_j)\, \zeta'_j \right), \end{aligned} \tag{1}$$

and, in the second equation, ζ_j and ζ'_j indicate the independent fading coefficients for the links between the receiver of interest and the nodes in the full-duplex cluster $\mathcal{C}_j$. Given the interference-limited nature of the networks under consideration, we disregard thermal noise and evaluate the performance of the system based on the signal-to-interference ratio (SIR). More specifically, in an effort to preserve the mathematical tractability of the problem, we are interested in the ratio between the incoming power of the desired signal at a receiver and the average value $\mathcal{I}$ of the interference it perceives. Within our framework, the latter quantity and its half- and full-duplex clusters induced components $\mathcal{I}_{\mathsf{hd}}$ and $\mathcal{I}_{\mathsf{fd}}$ can be expressed as

$$\mathcal{I} = \mathcal{I}_{\mathsf{hd}} + \mathcal{I}_{\mathsf{fd}} = \frac{1}{D} \int_0^D I_{\mathsf{hd}}(t)\, dt + \frac{1}{D} \int_0^D I_{\mathsf{fd}}(t)\, dt \tag{2}$$

The average signal-to-interference ratio for a half-duplex receiver thus readily follows as $\mathsf{SIR}_{\mathsf{hd}} = PL(r)\zeta/\mathcal{I}$. On the other hand, decoding during a full-duplex connection is also hampered by a residual self-interference component S due to imperfect cancellation algorithms, so that $\mathsf{SIR}_{\mathsf{fd}} = PL(r)\zeta/(\mathcal{I} + S)$. Buttressed by experimental results [4], we assume a linear dependence of S to the emitted power, and relate it to a cancellation efficiency coefficient $\eta \in [0, 1]$ as $S = P(1-\eta)$. This working hypothesis is particularly handy, as it induces SIR values which are

independent of P for both half- and full-duplex links, helping to identify broadly applicable tradeoffs. Accordingly, in the remainder of our discussion we will refer to the case of unit transmission power, and set $P = 1$ without loss of generality.

A threshold model is considered for decoding, with a packet being retrieved as soon as the average SIR experienced at its receiver is above a reference value θ. Focusing first on a half-duplex cluster, the probability of its data exchange to be successful directly follows:

$$p_s^{(\mathsf{hd})} = \Pr\{\mathsf{SIR}_{\mathsf{hd}} \geq \theta\} = \Pr\left\{\zeta \geq \frac{\theta\,(\mathcal{I}_{\mathsf{hd}} + \mathcal{I}_{\mathsf{fd}})}{L(r)}\right\} \tag{3}$$

Starting from the exponential distribution of ζ and leveraging the law of total probability over the two independent processes Λ_{hd} and Λ_{fd}, (3) can be conveniently written as

$$p_s^{(\mathsf{hd})} = \mathbb{E}\left[e^{-\mathcal{I}_{\mathsf{hd}}\,\theta\,r^{\alpha}}\right]\mathbb{E}\left[e^{-\mathcal{I}_{\mathsf{fd}}\,\theta\,r^{\alpha}}\right] = \mathcal{L}_{\mathcal{I}_{\mathsf{hd}}}(\theta r^{\alpha}) \cdot \mathcal{L}_{\mathcal{I}_{\mathsf{fd}}}(\theta r^{\alpha}) \tag{4}$$

where the second equality stems from the definition of Laplace transform of a random variable x, $\mathcal{L}_x(s) \triangleq \mathbb{E}[e^{-s\,x}]$. Following a similar approach, it is straightforward to also derive the success probability for a full-duplex link as

$$p_s^{(\mathsf{fd})} = e^{-(1-\eta)\theta r^{\alpha}} \cdot \mathcal{L}_{\mathcal{I}_{\mathsf{hd}}}(\theta r^{\alpha})\,\mathcal{L}_{\mathcal{I}_{\mathsf{fd}}}(\theta r^{\alpha}) = \beta\, p_s^{(\mathsf{hd})}, \tag{5}$$

where the factor

$$\beta \triangleq \exp\left(-(1-\eta)\theta r^{\alpha}\right).$$

accounts for imperfect self-interference cancellation.

In order to complement our analysis, we also evaluate the performance of the system in terms of the throughput density $\mathcal{T}$, defined as the average number of information bits per second successfully exchanged in the network per unit area. Assuming an information bitrate of W bit/s common to all transmissions, a delivered data unit contributes with WD bits to the throughput, so that $\mathcal{T}$ can be written in the form

$$\mathcal{T} = \lambda D\, W\left((1-q)p_s^{(\mathsf{hd})} + 2q\, p_s^{(\mathsf{fd})}\right) \tag{6}$$

Within (6), the first addend in brackets accounts for the fraction $1-q$ of half-duplex connections, delivering at most one data unit per link. As far as a two-way full-duplex link is concerned, instead, both packets exchanged between the involved nodes are delivered with probability $p_s^{(\mathsf{fd})} \cdot p_s^{(\mathsf{fd})}$, while only one of the two transmissions succeeds with probability $2p_s^{(\mathsf{fd})}(1-p_s^{(\mathsf{fd})})$. The average throughput contribution of a full-duplex cluster in terms of information units per link thus evaluates to $2p_s^{(\mathsf{fd})}$, as reported by the second addend in (6).

III. The Performance of Asynchronous Full-Duplex networks

The framework introduced in Section II highlights how the performance of the asynchronous system under consideration can be characterised as soon as the Laplace transforms $\mathcal{L}_{\mathcal{I}_{\mathsf{hd}}}(s)$ and $\mathcal{L}_{\mathcal{I}_{\mathsf{fd}}}(s)$ are known at $s = \theta r^{\alpha}$. An elegant formulation of the former was originally devised by Błaszczyszyn et al. in the context of purely half-duplex Aloha networks. For the sake of compactness we omit here the details of their derivation, referring the interested reader to the work in [23], and rather focus on a slightly modified version of the original outcome obtained via simple mathematical manipulations. Accordingly, we express the Laplace transform of the interference perceived at the typical receiver due to half-duplex pairs in the form

$$\mathcal{L}_{\mathcal{I}_{\mathsf{hd}}}\left(\theta r^{\alpha}\right) = \exp\Big(-4\lambda(1-q)\, D\, \Omega_{\mathsf{hd}}\Big), \tag{7}$$

where the ancillary function Ω_{hd} is defined as

$$\Omega_{\mathsf{hd}}(r,\theta,\alpha) = \pi r^2\, \theta^{\frac{2}{\alpha}}\, \Gamma\left(1+\frac{2}{\alpha}\right) \Gamma\left(1-\frac{2}{\alpha}\right) \frac{\alpha}{2(\alpha+2)} \tag{8}$$

and $\Gamma(x) = \int_0^{\infty} x^{t-1} e^{-x}\, dt$ is the complete Gamma function. The result in (7) is particularly insightful, as it isolates the role of two key performance drivers. On the one hand, an exponential dependence of $\mathcal{L}_{\mathcal{I}_{\mathsf{hd}}}$ – and thus of the success probability – on the duration D of the active links is prompted, stressing the intrinsic weakness of longer transmissions to interference. On the other hand, the factor Ω_{hd} summarises the impact of the system parameters r, θ and α, embedding the structure of the interference generated by half-duplex clusters.

Let us now focus instead on the contribution of full-duplex pairs. As a preliminary step, the average value of the generated interference $\mathcal{I}_{\mathsf{fd}}$ introduced in (2) can be conveniently simplified by recalling the definition in (1) to obtain

$$\mathcal{I}_{\mathsf{fd}} = \sum_{(\mathbf{u}_i, T_i) \in \Lambda_{\mathsf{fd}}} \omega(T_i) \cdot \big(L(\mathbf{u}_i)\, \zeta_i + L(\mathbf{v}_i)\, \zeta_i'\big),$$

where the time averaging is captured by the function

$$\omega(T_i) \triangleq \int_0^{D} \frac{\iota_i(t)}{D}\, dt = \begin{cases} \frac{D-|T_i|}{D} & T_i \in [-D, D] \\ 0 & \text{elsewhere} \end{cases}$$

Taking the lead from this, we can set the calculation of the the Laplace transform $\mathcal{L}_{\mathcal{I}_{\text{fd}}}(s),\ s \in \mathbb{R}$, in the form:

$$\mathcal{L}_{\mathcal{I}_{\text{fd}}}(s) = \mathbb{E}\Big[e^{-s\mathcal{I}_{\text{fd}}}\Big] = \mathbb{E}\left[\prod\nolimits_{\Lambda_{\text{fd}}} e^{-s\,\omega(T_i)(L(\mathbf{u}_i)\zeta_i + L(\mathbf{v}_i)\zeta_i')}\right] \tag{9}$$

The expectation in (9) operates both over fading and the PPP in its space and time components. As to the first, the independence of the involved Rayleigh channel coefficients allows to bring the expectation over random variables ζ_i and ζ_i' inside the product, enabling the reformulation reported in (10) at the bottom of the page. With reference to this, equality (a) simply follows by the law of the unconscious statistician, recalling that the fading coefficients are exponentially distributed with unit mean. On the other hand, step (b) is the application of Campbell's theorem to the homogeneous PPP Λ_{fd} of intensity λq [24], where $f(\mathbf{w})$ represents the generic probability distribution function over $\mathbb{R}^2$ of the second node of coordinates $\mathbf{v} = \mathbf{u}+\mathbf{w}$ in a full-duplex cluster (see Fig. 1). The formulation in (10) relates the Laplace transform to the averaging over the space and time components of a full-duplex cluster, and can be further simplified under the considered working assumptions. In particular, the linear trend and limited support of $\omega(T)$ lead via straightforward calculations to a closed-form expression for the inner integration:

$$\begin{aligned}&\int_{\mathbb{R}} \Big(1 - \int_{\mathbb{R}^2} \frac{1}{1+sL(\mathbf{u})\omega(T)} \frac{1}{1+sL(\mathbf{u}+\mathbf{w})\omega(T)} f(\mathbf{w})d\mathbf{w}\Big) dT \\ &= 2D \int_{\mathbb{R}^2} 1 - \frac{\ln\big(1+sL(\mathbf{u})\big) - \ln\big(1+sL(\mathbf{u}+\mathbf{w})\big)}{s\big(L(\mathbf{u})-L(\mathbf{u}+\mathbf{w})\big)} f(\mathbf{w})d\mathbf{w}\end{aligned} \tag{11}$$

Plugging (11) into (10), the remaining spatial averaging can be conveniently expressed resorting to polar coordinates and recalling how $f(\mathbf{w})$ describes a uniform distribution over a circle of radius r center at $\mathbf{u}$, so that $\mathbf{w} = r\,e^{-j\varphi}$. Finally, observing that the overall integrand does not

---

$$\begin{aligned}\mathcal{L}_{\mathcal{I}_{\text{fd}}}(s) &= \mathbb{E}_{\Lambda_{\text{fd}}}\left[\prod\nolimits_{\Lambda_{\text{fd}}} \mathbb{E}_{\zeta_i}\left[e^{-s\omega(T_i)L(\mathbf{u}_i)\zeta_i}\right] \mathbb{E}_{\zeta_i'}\left[e^{-s\omega(T_i)L(\mathbf{v}_i)\zeta_i'}\right]\right] \\ &\overset{(a)}{=} \mathbb{E}_{\Lambda_{\text{fd}}}\left[\prod\nolimits_{\Lambda_{\text{fd}}} \frac{1}{1+sL(\mathbf{u}_i)\omega(T_i)} \cdot \frac{1}{1+sL(\mathbf{v}_i)\omega(T_i)}\right] \\ &\overset{(b)}{=} \exp\left(-\lambda q \int_{\mathbb{R}^2} d\mathbf{u} \int_{\mathbb{R}} dT \left(1 - \int_{\mathbb{R}^2} \frac{1}{1+sL(\mathbf{u})\omega(T)} \frac{1}{1+sL(\mathbf{u}+\mathbf{w})\omega(T)} f(\mathbf{w})d\mathbf{w}\right)\right)\end{aligned} \tag{10}$$

depend on the azimuthal component of the cluster center due to symmetry, we get to the sought result

$$\mathcal{L}_{\mathcal{I}_{\mathsf{fd}}}(\theta r^{\alpha}) = \exp\Big(-4\lambda q\, D\, \Omega_{\mathsf{fd}}\Big), \tag{12}$$

where Ω_{fd} is reported by (13) at the bottom of the page.

The presented result is remarkable, as we can once more isolate the effect of the key design parameters q and D from the factor Ω_{fd}. The latter, in turn, is not affected by the fraction of full-duplex clusters in the network nor by the duration of the transmissions, but rather only characterises the interference contribution that each full-duplex link produces. In this perspective, further insights are offered by the following characterisation of Ω_{fd}, whose proof is reported in Appendix A:

Theorem 1: Under the assumptions of the presented framework, for any $\alpha > 2$ and $r \geq 1$, it holds

$$\Omega_{\mathsf{fd}}(r,\theta,\alpha) = \delta(\theta,\alpha)\cdot\Omega_{\mathsf{hd}}(r,\theta,\alpha) \tag{14}$$

The statement of Theorem 1 clarifies how the ratio $\Omega_{\mathsf{fd}}/\Omega_{\mathsf{hd}}$ is in fact independent of the distance r between two nodes within a cluster, and entails two relevant remarks. In the first place, recalling the expression of Ω_{hd} in (8), we infer that the Laplace transform of the average interference generated by full-duplex pairs exhibits a quadratic dependence on r as well. Thus, the success probability of a half-duplex data exchange is in the form of an exponential function of r^2 regardless of the path loss exponent α. Even more interestingly, under the assumption of perfect self-interference cancellation, i.e., $\beta = 1$,the same trend holds for $p_s^{(\mathsf{fd})}$, leading to the conclusion that the performance ratio between between half- and full-duplex links is not affected by the link distance. Such a result is partly counter-intuitive, as one may expect the latter to be more failure-prone for father away source-destination pairs, and will be discussed in more details later. Secondly, the expression in (14) is particularly handy, since it allows to compute Ω_{fd} as

$$\Omega_{\mathsf{fd}}(r,\theta,\alpha) = \int_0^{\infty} u \left(\pi - \int_0^{\pi} \frac{\ln\left(1+\theta r^{\alpha} u^{-\alpha}\right) - \ln\left(1+\theta r^{\alpha}\left(u^2+r^2+2ru\cos\varphi\right)^{-\frac{\alpha}{2}}\right)}{\theta r^{\alpha}\left(u^{-\alpha}-\left(u^2+r^2+2ru\cos\varphi\right)^{-\frac{\alpha}{2}}\right)} d\varphi \right) du \tag{13}$$

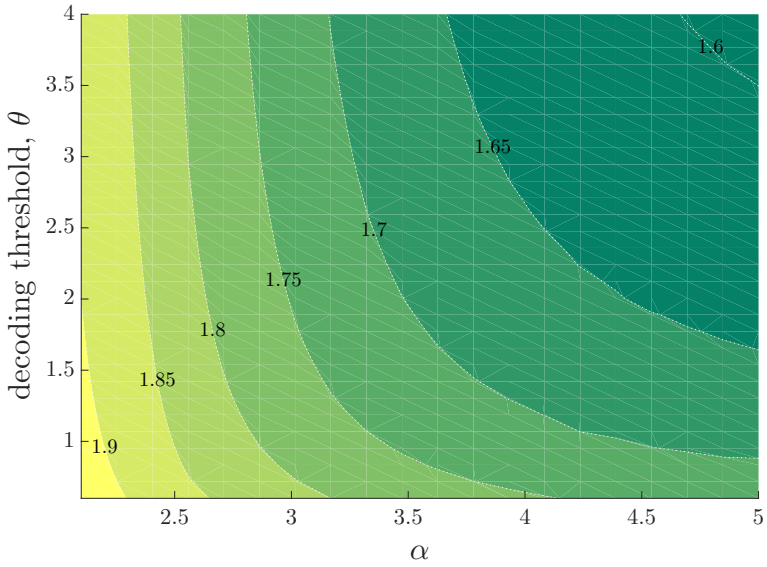

Fig. 2: Values of $\delta(\theta, \alpha) = \Omega_{\mathsf{fd}}(r, \theta, \alpha)/\Omega_{\mathsf{hd}}(r, \theta, \alpha)$ as a function of the path loss exponent α and of the decoding threshold θ.

the product of Ω_{hd}, for which a simple closed form expression is available, and of the function δ which can readily be evaluated numerically. Furthermore, δ only depends on the decoding threshold and on the path loss exponent, so that it is sufficient to compute it once for a (θ, α) pair to readily get in closed form the success probabilities for any value of density λ, for any fraction of full-duplex clusters as well as for any link distance. The introduced framework thus offers a compact tool to easily characterise the performance of a variety of network configurations. Along this line of reasoning, Fig. 2 reports in contour form the values of $\delta(\theta, \alpha)$ for an extensive set of parameters. In order to get a deeper understanding of the plot, it is insightful to consider the two opposite scenarios of a purely half-duplex, i.e., $q = 0$, and a purely full-duplex, i.e., $q = 1$, network. Recalling (4), the success probability for a data exchange in the former case simplifies to $p_s^{(\mathsf{hd})} = \exp(-4\lambda D \Omega_{\mathsf{hd}})$. Similarly, when $q = 1$, we get from (5) and under the hypothesis of ideal self-interference cancellation $p_s^{(\mathsf{fd})} = \exp(-4\lambda D \Omega_{\mathsf{fd}})$. Assuming the same configuration in terms of traffic intensity λ and packet duration D, thus, the reliability loss undergone in a solely full-duplex system due to the higher interference triggered by concurrent communications between nodes of a cluster is driven exactly by the ratio δ. From this standpoint, Fig. 2 quantifies two interesting trends. On the one hand, larger path loss exponents are especially beneficial to

full-duplex communications, by virtue of the stronger attenuation undergone by the aggregate network interference. On the other hand, for a given value of α, the same reduction in terms of θ, i.e., the same improvement in decoding schemes to tolerate lower SIR, pays off more in a completely half-duplex configuration than in a purely full-duplex one, as in the latter the beneficial effect of more advanced receivers is counteracted by the additional interference that has to be faced.

The closed-form expressions derived for the packet retrieval probabilities finally allow us to evaluate the network throughput density, which offers a more comprehensive characterisation of the overall system performance by capturing the tradeoff between spatial reuse and additional interference triggered by in-band full-duplex. In particular, the general formulation of (6) can now be further elaborated to obtain

$$\mathcal{T} = W\lambda D\big(1+q\,(2\beta-1)\big)\cdot\exp\Big(-4\lambda D\big((1-q)\Omega_{\mathsf{hd}}+q\Omega_{\mathsf{fd}}\big)\Big) \tag{15}$$

Within (15), we can conveniently introduce the channel load $\mathsf{G} = \lambda D$, quantifying for an unslotted network the average the fraction of time the medium is occupied over a reference unit area. Leaning on this definition, it is interesting to notice how, despite the non-trivial nature of the system under study, the throughput exhibits the trend of a typical Aloha-based MAC, mathematically described by the product of G to a negative exponential function of G itself. However, throughout our analysis we do not characterise performance in terms of channel load, but rather investigate the behaviour of the network under a fixed traffic density λ and varying the duration of D of a data exchange. The rationale behind this choice is twofold. In the first place, the followed approach will offer insightful hints on how to optimise systems in which topology and traffic pattern cannot be controlled. A relevant example are MTC networks, where each node of a vast population only sporadically generates a packet, so that identifying the proper length of an information unit for a half- or full-duplex exchange can become of critical relevance. Secondly, capturing the dependence of the throughput on D will pave the road to the investigation of an additional degree of freedom that is typically missing in slotted systems carried out in Section IV, where packets of different durations will be considered.

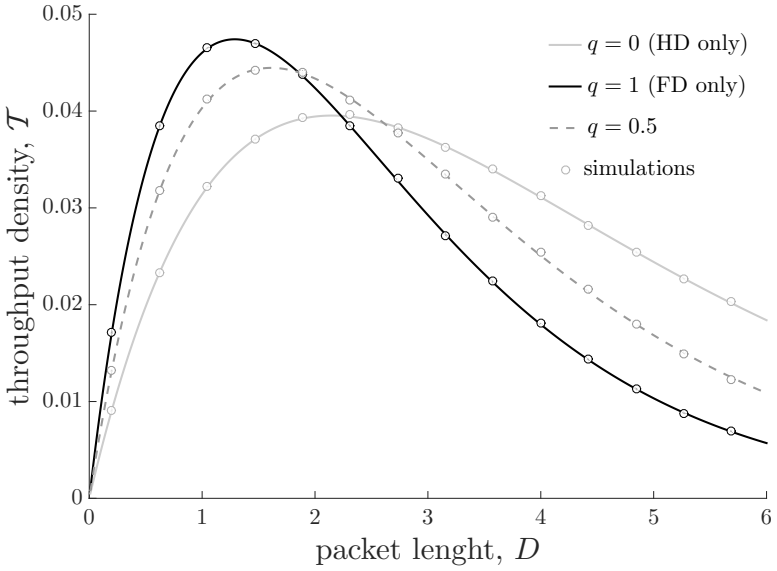

Fig. 3: Network throughput density vs packet length for different fractions of full-duplex clusters. Lines indicate the analytical trends, whereas circled markers the results of Monte Carlo simulations.

A. On the optimal fraction of FD links

Starting from these remarks, let us begin our discussion by assuming ideal self-interference cancellation (i.e., $\eta = 1$), and focus on the two cases of a purely half-duplex and a purely full-duplex network. Unless otherwise specified, we refer to a system with parameters $\lambda = 0.05$, $r = 1$, $\alpha = 4$, $W = 1$ and $\theta = 2$. The throughput density achievable in the two cases when varying the packet length D is reported by solid lines in Fig. 3, together with results obtained via Monte Carlo simulations of the described time-space PPP that validate the framework. The plot clearly highlights how, for short data units, full-duplex capabilities indeed boost performance, thanks to the higher degree of spatial reuse they enable. On the other hand, when longer packets are considered, the detrimental effect of the additional interference generated by having two concurrent transmissions per cluster kicks in, leading to a steep decrease in the achievable throughput and eventually making a simple half-duplex setting more convenient. Leveraging the broad applicability of (15), Fig. 3 also depicts the behaviour of a hybrid system in which only half the pairs are capable of transmitting and receiving at the same time ($q = 0.5$, dashed line). As expected, such a configuration blends benefits and drawbacks identified for the $q = 0$ and $q = 1$ cases, improving over a purely half-duplex system for short communications and degrading

more gently than the full-duplex only scheme for longer information units. More interestingly, the curves also prompt a third region in which an intermediate configuration outperforms in fact both its counterparts. This observation raises then the relevant question of what is the fraction q^* of full-duplex clusters one should aim for to maximise throughput given a certain value of D. On the one hand, if we naturally interpret q as the penetration level of more advanced terminals in a traditional half-duplex network, the optimisation problem can be seen as a driver in the decision on whether to undergo the costs to further upgrade an existing system. On the other hand, even when the capabilities of deployed nodes cannot be changed, q may still represent a key design parameter to tweak the fraction of links that shall in fact resort to full-duplex to leverage the non-trivial tradeoff between spatial reuse and additional interference at its utmost. The question can be effectively addressed leaning on the simple structure of (15), and recalling that Ω_{hd} and Ω_{fd} do not depend on q. Setting then $\partial\mathcal{T}/\partial q = 0$, we obtain the optimal fraction of full-duplex clusters when varying D:

$$q^* = \begin{cases} 1 & D \in [0, D_1) \\ \dfrac{1}{4\lambda(\Omega_{\mathsf{fd}} - \Omega_{\mathsf{hd}})} - \dfrac{1}{2\beta - 1} & D \in [D_1, D_2) \\ 0 & D \geq D_2 \end{cases} \tag{16}$$

where the switching boundaries are defined as

$$D_1 = \frac{2\beta - 1}{4\lambda(\Omega_{\mathsf{fd}} - \Omega_{\mathsf{hd}})} \cdot \left(1 - \frac{1}{2\beta}\right), \quad D_2 = \frac{2\beta - 1}{4\lambda(\Omega_{\mathsf{fd}} - \Omega_{\mathsf{hd}})} \tag{17}$$

Confirming the intuition prompted by Fig. 3, (16) identifies three optimal operating regions, reported graphically in Fig. 4 under the assumption of perfect self-interference cancellation. For sufficiently short packets ($D \leq D_1$), network throughput is indeed maximised by letting as many clusters as possible – ideally, all of them – operate in full-duplex mode. Conversely, when data units are longer than threshold D_2, even full-duplex capable nodes shall not take advantage of simultaneous transmission and reception in favour of unidirectional links. Remarkably, a closed form expression is available to also characterise the optimal value q^* in the intermediate region as a function of the ancillary functions Ω_{fd} and Ω_{hd}. The plot thus presents a first design takeaway, suggesting the use of in-band full-duplex for quick information exchanges between two nodes rather than for longer connections. Such traffic patterns in turn are of strong interest, being well matched by an increasing number of applications that embody the small-data

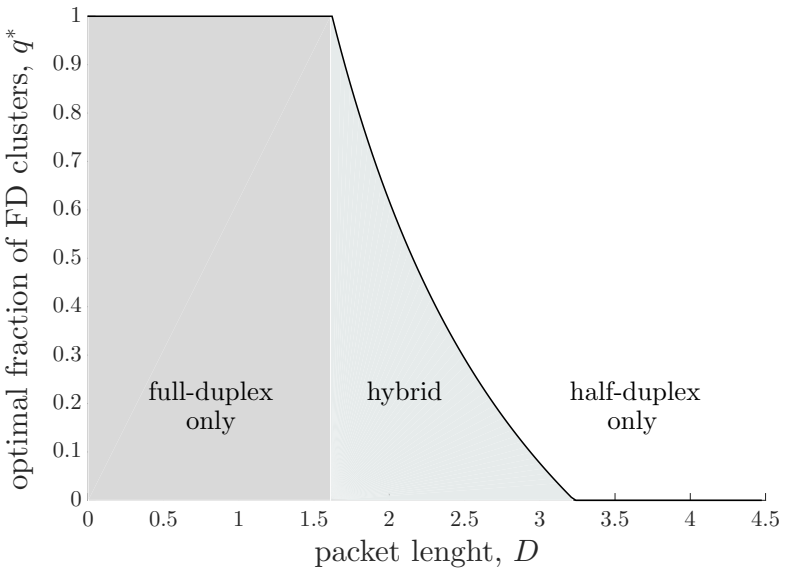

Fig. 4: Fraction of full-duplex clusters to maximise network throughput vs. packet length. Perfect self-interference cancellation is assumed.

paradigm [22], and representing a core aspect in the domain of machine-type and device-to-device communications which typically generate short and sporadic data units. Even more relevant is to stress that the optimal working regions introduced in Fig. 4 describe the network behaviour assuming terminals capable of ideally removing any trace of self-interference. The performance deterioration undergone by full-duplex when exchanging long data units, thus, cannot be eased resorting to more advanced signal processing, but rather represents an intrinsic and fundamental limitation faced by this technology in large and asynchronous networks.

In parallel to this general bound, the optimisation problem solved in (16)-(17) also offers a deeper understanding of the traffic patterns suitable for full-duplex in practical implementations, encompassing the impact of imperfect interference cancellation via the factor β. The outcome of the study is reported in Fig. 5, where the dashed line reproduces for completeness the regions under ideal cancellation discussed so far, whereas solid lines depict the q^* against D curve for different values of the efficiency parameter η. A critical role for residual self-interference decidedly emerges from the plot, as lower values of η progressively limit the region of convenience for solely full-duplex systems to shorter communications. This trend eventually leads, for $\beta \geq 1/2$, to a situation in which a simpler half-duplex network offers better

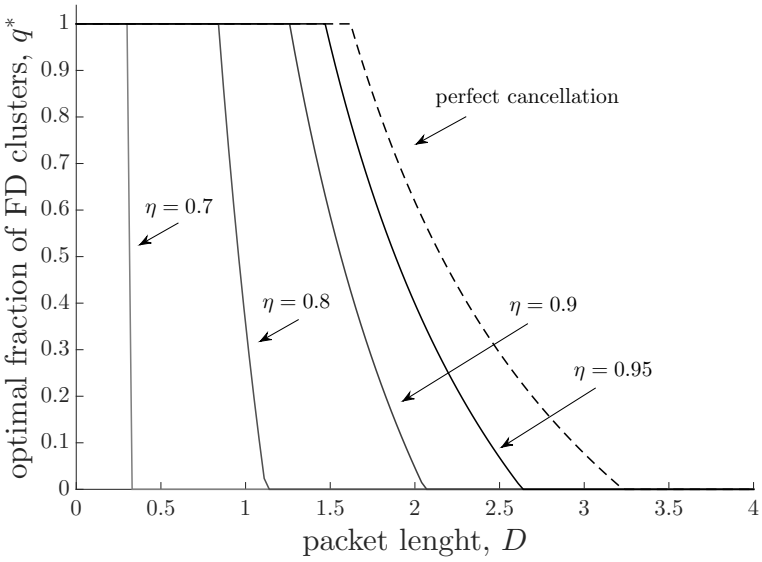

Fig. 5: Optimal fraction of full-duplex clusters to maximise network throughput vs. packet length. Imperfect self-interference cancellation is considered.

performance regardless of the packet duration. Recalling the definition of β, this translates into a minimum requirement in terms of cancellation efficiency for full-duplex to be useful in a distributed asynchronous network in the form $\eta \geq 1 - \ln(2) r^{-\alpha}/\theta$. As a second remark, we notice that the presence of residual self-interference induces sharper transitions between the regions where only full- and only half-duplex are to be preferred. Such a trend is in general not desirable, as the operating condition of most interest is exactly the one where both kinds of link coexist. From this standpoint, not only can intermediate values of q be interpreted as representative of networks where a portion of the terminals have full-duplex capabilities, but also of topologies in which nodes within a cluster do not always have traffic for each other, failing the fundamental condition for a bidirectional connection to be established in the first place.

B. On the maximum achievable FD gain

The analysis carried out so far has clarified the importance of carefully selecting how many full-duplex links to trigger. We now extend our study by tackling a complementary task, and identifying how to tune the duration of data exchanges given a certain network configuration in terms of q so to maximise performance. The solution to this problem directly follows from the

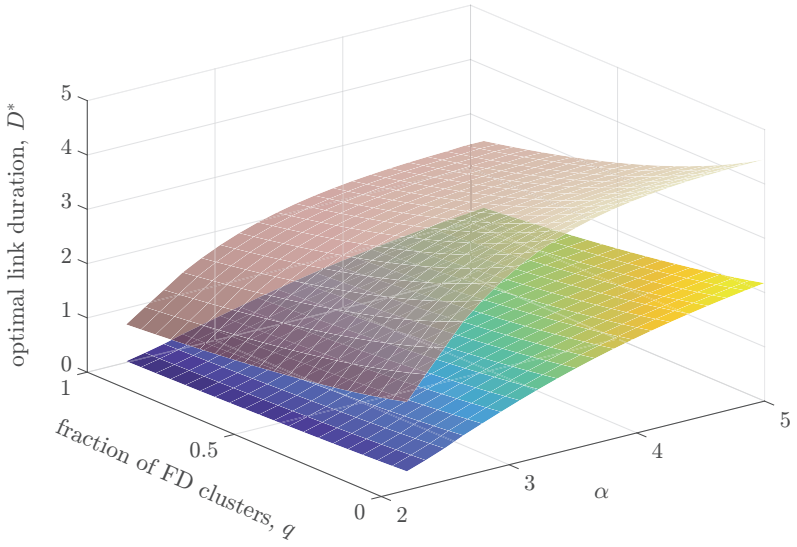

Fig. 6: Optimal link duration as a function of the fraction of full-duplex clusters and of the path-loss exponent α. The upper surface reports the case of decoding threshold $\theta = 0.5$, whereas the lower one describes the behaviour for $\theta = 3$. $r = 1$, $\lambda = 0.05$.

simple dependence of $\mathcal{T}$ on the packet length D reported in (15). Straightforward calculations allow to derive the optimal working point D^* yielding the peak throughput density in the form

$$D^* = \frac{1}{4\lambda\Big((1-q)\,\Omega_{\mathsf{hd}} + q\,\Omega_{\mathsf{fd}}\Big)} \tag{18}$$

Remarkably, the expression in (18) does not depend on the efficiency of self-interference cancellation, and thus offers once more a broadly applicable result that stems from the very structure of the interference generated by half- and full-duplex clusters embedded into the ancillary Ω functions. On the other hand, the optimal working point is determined, for a given traffic intensity λ,[3] by the triplet (r, θ, α). Let us first focus on the role played by the last two parameters and refer to the results reported in Fig. 6, which presents the optimal link duration D^* as a function of α for different values of q and $r = 1$. The lower surface characterises the case $\theta = 3$, whereas the upper one focuses on the scenario with decoding threshold set to 0.5. Under both configurations, the optimal working region shifts towards shorter communications for networks with higher

[3]Note that the maximisation problem could also be carried out over the channel load, leading to a scaled result in the form $\mathsf{G}^* = \lambda D^*$. The outcomes of the following discussion thus also directly apply to load optimisation.

penetration level of full-duplex clusters. Such a trend, in accordance to what discussed so far, derives from the higher efficiency of bidirectional links with smaller data units, and extends the presented design hints to a broader set of system and environmental setups. Secondly, moving along the α-axis, we observe how a stronger path loss enables to effectively sustain higher channel loads due to the sharper attenuation undergone by interfering signals.[4] More interestingly, the effect becomes less pronounced for larger values of q, being counterbalanced by the additional interference induced by bidirectional communications. As to the dependence of D^* on the decoding threshold, the plot presents two quite distinct configurations. The former ($\theta = 0.5$), models decoders as capable of retrieving the information unit of interest even when interference is higher than the incoming power from the cluster companion, and is representative of systems that employ advanced signal processing solutions or spread spectrum [25]. The latter, in turn, focuses on receivers that leverage the capture effect to synchronise to (and potentially decode) a packet only if its power exceeds the aggregate level of the concurrently active links. As expected, lower values of θ favour an effective operation of the system resorting to longer information exchanges, with the effect becoming more pronounced in networks that exhibit a lower fraction of full-duplex clusters due to the lower experienced interference.

The results presented in Fig. 6 provide useful insights on how to tune system parameters in order for the network to work under optimal channel load. On the other hand, the developed framework also allows to address the perhaps more relevant aspect of how such operating conditions reflect in terms of actual performance. In this perspective, plugging (18) into (15), the maximum network throughput density $\mathcal{T}^*$ achievable by a network with a fraction q of full-duplex clusters evaluates to

$$\mathcal{T}^* = \frac{W\big(1+q(2\beta-1)\big)}{4e\big((1-q)\,\Omega_{\mathsf{hd}}+q\,\Omega_{\mathsf{fd}}\big)} \tag{19}$$

Assuming the possibility of properly setting the communications parameters, we can thus understand what is the maximum gain that in-band bidirectional links can award when articulated topologies are considered. To this aim, we introduce the ratio χ of the peak throughput of a solely full-duplex network to the same quantity for a network operated in half-duplex mode, and

[4]For the case under analysis $r = 1$, so that the useful incoming power at a receiver is not affected by a change in the path-loss coefficient.

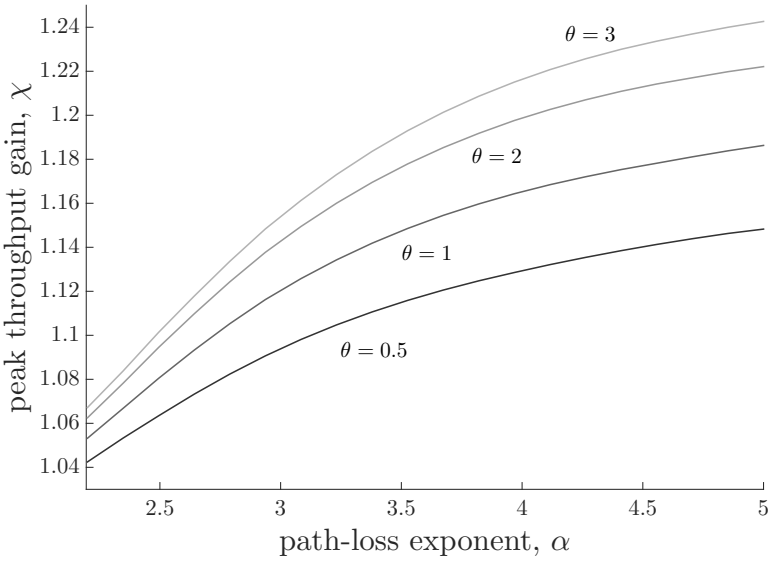

Fig. 7: Peak throughput gain achievable by a purely full-duplex network over a solely half-duplex one vs path-loss exponent. Perfect self-interference cancellation is assumed.

readily get from (19)

$$\chi \triangleq \frac{\max\left\{\mathcal{T} \,|\, q=1\right\}}{\max\left\{\mathcal{T} \,|\, q=0\right\}} = 2\beta \cdot \frac{\Omega_{\mathsf{hd}}}{\Omega_{\mathsf{fd}}}$$

Remarkably, the obtained expression is independent of λ, showing how the maximum gain brought by spatial reuse is intrinsically limited by the nature of the interference generated by full-duplex links and does not scale with the density of the population. Moreover, χ is conveniently expressed as twice the correction factor $\Omega_{\mathsf{hd}}/\Omega_{\mathsf{fd}} = 1/\delta$, which is lower than one even under the assumption of ideal self-interference cancellation. Not only does this confirms that full-duplex can in fact not double the network capacity in large and completely uncoordinated systems, but also readily quantifies the obtainable improvement. In fact, if we initially consider the ideal case $\beta = 1$, χ is completely defined by the ancillary function $\delta(\theta, \alpha)$ introduced and already discussed in Fig. 2. For the sake of readability, the behaviour of χ against α for different values of the decoding threshold θ is also explicitly reported in Fig. 7. Recalling the outcome of Theorem 1 we can immediately infer that, under the assumption of perfect self-interference cancellation, χ is independent of the link distance r. The results being presented are thus broadly applicable and characterise the fundamental behaviour of full-duplex systems, whose increased spatial reuse can

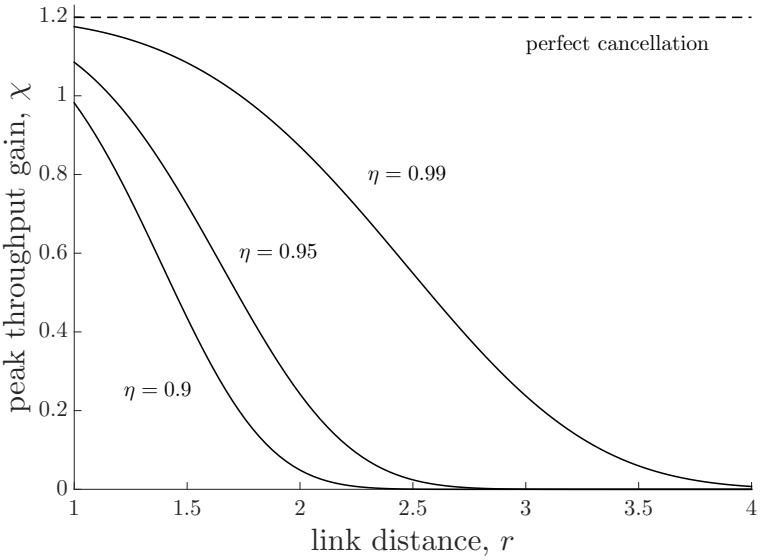

Fig. 8: Peak throughput gain achievable by a purely full-duplex network over a solely half-duplex one vs link distance.

pay off with at most a 20% throughput gain over their half-duplex counterparts for the reference parameter set $\alpha = 4, \theta = 2$.

On the other hand, the situation drastically changes when imperfect cancellation is brought into the picture. By virtue of the exponential dependence of β on the cluster radius, indeed, residual self-interference induces a dramatic degradation of the throughput gain offered by spatial reuse. This aspect is highlighted in Fig. 8, which reports χ as a function of r, and shows how already small losses in η fundamentally limit the throughput of the full-duplex network. Even more interestingly, poorer interference cancellation levels (e.g., $\eta \leq 0.9$ in our case) eventually lead to a condition in which a purely half-duplex network outperforms its full-duplex counterpart regardless of the proximity of the communicating nodes. This offers two relevant design take-aways. In the first place, not only shall full-duplex links be employed when short data units have to be exchanged, but also they shall carefully be triggered when source and addressee are sufficiently close to each other. Secondly, the potential improvement in terms of capacity shall not distract from the importance of achieving levels of self-interference cancellation even stronger than what desirable from an isolated-link viewpoint. In the quest for low-cost terminals, this may in fact constitute a crucial challenge.

IV. The Impact of different Packet Durations

The framework developed in Section III extensively characterises the performance of an Aloha network with full-duplex capabilities when all transmissions occupy the channel for the same time. On the other hand, one of the key outcomes of the study has been exactly to stress how half- and full-duplex links exhibit quite distinct requirements in terms of packet duration to operate optimally, with the former supporting longer communications and the latter leveraging spatial reuse at its utmost when exchanging short information units. Such a remark triggers the natural question of whether and how the system may benefit by independently tuning the duration of links of different nature. Notably, not only would the answer pave the road for additional optimisations, but also it would shed further light on the differences between asynchronous full-duplex systems and their slotted counterparts, clarifying the role of the additional degree of freedom represented by variable packet lengths for the former family.

We then tackle the problem by extending the presented analysis, and focus on networks where each half-duplex connection has duration D, while a full-duplex exchange occupies the medium for γD seconds. For consistency, we evaluate performance in terms of the throughput density $\mathcal{T}$ introduced in (6), which readily extends in this case to

$$\mathcal{T} = \lambda W D \Big((1-q) p_s^{(\mathsf{hd})} + 2\gamma q p_s^{(\mathsf{fd})} \Big) \tag{20}$$

The key task is thus once again to study the decoding probability for the different types of data exchanges. From this standpoint, even though the computational approach followed in Section II still holds and allows to express the success rate as the product of two Laplace transforms, the new setting slightly modifies the meaning of the involved factors. If we focus on a bidirectional connection, reception of incoming data is in the first place hampered by concurrent transmissions of clusters also operating in full-duplex mode with the same packet length. The impact of this interference contribution on the success probability is exactly the one captured by the Laplace transform in (12), considering data transfers of γD seconds. Conversely, the result derived in (7) does not accounts properly for the impact of half-duplex connections whose duration is different from the one of the information unit being decoded, and needs to be extended. A similar reasoning applies to the success probability of a half-duplex link, making it possible to rely on the Laplace transform of the interference generated by clusters of the same kind in (7) while requiring a new computation for the impact of full-duplex communications with different

duration. In summary, we have

$$p_s^{(\mathsf{hd})} = \mathcal{L}_{\mathcal{I}_{\mathsf{hd}}}\big(\theta r^\alpha, D\big)\,\mathcal{L}_{\mathcal{I}_{\mathsf{fd,hd}}}\big(\theta r^\alpha\big) \tag{21}$$

$$p_s^{(\mathsf{fd})} = \mathcal{L}_{\mathcal{I}_{\mathsf{fd}}}\big(\theta r^\alpha, \gamma D\big)\,\mathcal{L}_{\mathcal{I}_{\mathsf{hd,fd}}}\big(\theta r^\alpha\big)\cdot\beta \tag{22}$$

where the first factors in (21) and (22) are the Laplace transforms derived in Section III with an additional argument specifying the packet duration that shall be accounted for in the corresponding exponential function; $\mathcal{L}_{\mathcal{I}_{\mathsf{fd,hd}}}$ accounts for the interference generated by full-duplex links of duration γD over a half-duplex reception; and $\mathcal{L}_{\mathcal{I}_{\mathsf{hd,fd}}}$ covers the interference affecting a full-duplex receiver due to half-duplex clusters transmitting for D seconds.

Let us initially focus on the last term. By definition, and following the same steps discussed for the derivation of (10), we can write

$$\begin{aligned}\mathcal{L}_{\mathcal{I}_{\mathsf{hd,fd}}}(s) &= \mathbb{E}\Big[\prod\nolimits_{\Lambda_{\mathsf{hd}}} e^{-s\omega'(T_i,\gamma)L(\mathbf{u}_i)\zeta_i}\Big] \\ &= \exp\left(-\lambda(1-q)\int_{\mathbb{R}^2} d\mathbf{u}\int_{\mathbb{R}}\left(1-\frac{1}{1+sL(\mathbf{u})\omega'(T,\gamma)}\right)dT\right)\end{aligned} \tag{23}$$

where the ancillary function reporting for the fraction of the half-duplex transmission of cluster $\mathcal{C}_i$ overlapping with the bidirectional link of interest is slightly reformulated to account for the different durations as

$$\omega'(T_i,\gamma) \triangleq \frac{1}{\gamma D}\int_0^{\gamma D} \mathbb{1}(T_i \le t \le T_i + D)\,dt$$

If we concentrate for the moment on the scenario $\gamma \le 1$, simple calculations show that ω' has support $[-D, \gamma D]$ and evaluates within it to

$$\omega'(T_i, \gamma \le 1) = \frac{1}{\gamma D}\cdot\begin{cases} D+T_i & T_i \in [-D, -D(1-\gamma)) \\ \gamma D & T_i \in [-D(1-\gamma), 0) \\ \gamma D - T_i & T_i \in [0, \gamma D] \end{cases}$$

This outcome allows us to explicitly solve the time integral in (23), which can be expressed as

$$2\gamma D\left(1-\frac{\ln(1+sL(\mathbf{u}))}{sL(\mathbf{u})}+\frac{1-\gamma}{2\gamma}\left(1-\frac{1}{1+sL(\mathbf{u})}\right)\right) \tag{24}$$

Finally, plugging (24) into (23) and observing that the integration over the spatial component is independent of the angular coordinate of the interfering half-duplex cluster, it is possible to

derive a closed form expression for the sought Laplace transform:

$$\mathcal{L}_{\mathcal{I}_{\mathsf{hd,fd}}}(\theta r^{\alpha}|\gamma \leq 1) = \exp\Big(-4\lambda(1-q)\gamma D\,\Omega'_{\mathsf{hd}}\Big), \tag{25}$$

resorting once more to the auxiliary function

$$\Omega'_{\mathsf{hd}}(r,\theta,\alpha\,|\gamma \leq 1) = \pi r^2\theta^{\frac{2}{\alpha}}\Gamma\left(1+\frac{2}{\alpha}\right)\Gamma\left(1-\frac{2}{\alpha}\right)\left(\frac{\alpha}{2(2+\alpha)}+\frac{1-\gamma}{2\gamma}\right) \tag{26}$$

The achieved result is quite insightful, as it provides a neat extension of the reference case studied in Section III. Firstly, comparing (25) to the Laplace transform of half-duplex interference reported in (7), we infer that the role played by the packet length D and the traffic density λ is decoupled from the the other system parameters even when links of different durations are allowed in the network. Even more interestingly, (26) captures the effect of longer half-duplex communications over a full-duplex data exchange with respect to its counterpart in (8) simply by means of an additive correction factor embodied by the term $(1-\gamma)/2\gamma$.

To complete the performance characterisation in terms of success probability, the evaluation of the impact of interference generated by full-duplex pairs – quantified by $\mathcal{L}_{\mathcal{I}_{\mathsf{fd,hd}}}$ – is in order. Considering again the case $\gamma \leq 1$, the definition of Laplace transform leads us to

$$\mathcal{L}_{\mathcal{I}_{\mathsf{fd,hd}}}(s) = \mathbb{E}\Big[\prod\nolimits_{\Lambda_{\mathsf{fd}}} e^{-s\omega''(T_i,\gamma)(L(\mathbf{u}_i)\zeta_i + L(\mathbf{v}_i)\zeta'_i)}\Big],$$

where the auxiliary function ω'' expresses the average fraction of the half-duplex reception interfered by the full-duplex transmissions in cluster $\mathcal{C}_i$ as

$$\omega''(T_i,\gamma) \triangleq \frac{1}{D}\int_0^D \mathbb{1}(T_i \leq t \leq T_i+\gamma D)\,dt \tag{27}$$

(27) paves the road for the mathematical derivation of $\mathcal{L}_{\mathcal{I}_{\mathsf{fd,hd}}}$, which proceeds along the same footsteps taken in Section III. While conceptually similar, the involved calculations are rather cumbersome, all the more so if we observe that for $\gamma > 1$ slightly different structures are obtained for the ω' and ω'' functions, prompting further integrations to be tackled. For the sake of compactness we thus omit the details of the derivation, and report here the key result, eventually expressing the success probabilities in a network with half- and full-duplex links of duration D and γD seconds respectively as

$$p_s^{(\mathsf{hd})} = \exp\Big(-4\lambda D\Big((1-q)\,\Omega_{\mathsf{hd}} + q\,\Omega'_{\mathsf{fd}}\Big)\Big)$$

$$p_s^{(\mathsf{fd})} = \beta\cdot\exp\Big(-4\lambda\gamma D\Big((1-q)\,\Omega'_{\mathsf{hd}} + q\,\Omega_{\mathsf{fd}}\Big)\Big)$$

Here, Ω_{hd} and Ω_{fd} are the functions already discussed in (8) and (13), whereas Ω'_{hd} and Ω'_{fd} are summarised for any value of γ in equations (29)-(30). For completeness, we also include in (28) the explicit structure of the ancillary functions $\omega'(t,\gamma)$ and $\omega''(t,\gamma)$ which are used to solve the integrals leading to the Laplace transforms.

The presented framework extension enables thus a direct comparison to the reference case discussed in the initial part of the paper. A first question of interest is whether and how much one could gain by letting half- and full-duplex connections have different durations. To gather

$$\omega'(T_i,\gamma\leq 1)=\frac{1}{\gamma D}\cdot\begin{cases} D+T_i & T_i\in[-D,-D(1-\gamma)) \\ \gamma D & T_i\in[-D(1-\gamma),0) \\ \gamma D-T_i & T_i\in[0,\gamma D] \end{cases} \qquad \omega'(T_i,\gamma>1)=\frac{1}{\gamma D}\cdot\begin{cases} D+T_i & T_i\in[-D,0) \\ D & T_i\in[0,D(\gamma-1)) \\ \gamma D-T_i & T_i\in[D(\gamma-1)),\gamma D] \end{cases}$$

$$\omega''(T_i,\gamma\leq 1)=\frac{1}{D}\cdot\begin{cases} \gamma D+T_i & T_i\in[-\gamma D,0) \\ \gamma D & T_i\in[0,D(\gamma-1)) \\ \gamma D-T_i & T_i\in[D(\gamma-1),D] \end{cases} \qquad \omega''(T_i,\gamma>1)=\frac{1}{D}\cdot\begin{cases} \gamma D+T_i & T_i\in[-D\gamma,-D(\gamma-1)) \\ D & T_i\in[-D(\gamma-1),0) \\ \gamma D-T_i & T_i\in[0,D] \end{cases} \tag{28}$$

$$\begin{aligned} \Omega'_{\mathsf{hd}}(r,\theta,\alpha|\gamma\leq 1)&=\pi r^2\theta^{\frac{2}{\alpha}}\Gamma\left(1+\frac{2}{\alpha}\right)\Gamma\left(1-\frac{2}{\alpha}\right)\left(\frac{\alpha}{2(2+\alpha)}+\frac{1-\gamma}{2\gamma}\right) \\ \Omega'_{\mathsf{hd}}(r,\theta,\alpha|\gamma>1)&=\pi r^2\theta^{\frac{2}{\alpha}}\Gamma\left(1+\frac{2}{\alpha}\right)\Gamma\left(1-\frac{2}{\alpha}\right)\left(\frac{\alpha}{2(2+\alpha)}+\frac{\gamma-1}{4\gamma}\right)\gamma^{-(1+2/\alpha)} \end{aligned} \tag{29}$$

$$\Omega'_{\mathsf{fd}}(r,\theta,\alpha|\gamma\leq 1)=\int_0^\infty u\left(\frac{\pi(1+\gamma)}{2}-\int_0^\pi\frac{\ln\left(\frac{1+\gamma\theta r^\alpha u^{-\alpha}}{1+\gamma\theta r^\alpha\ell(u,\varphi)}\right)}{\theta r^\alpha\left(u^{-\alpha}-\ell(u,\varphi)\right)}-\frac{1-\gamma}{2(1+\gamma\theta r^\alpha u^{-\alpha})(1+\gamma\theta r^\alpha\ell(u,\varphi))}d\varphi\right)du$$

$$\Omega'_{\mathsf{fd}}(r,\theta,\alpha|\gamma>1)=\int_0^\infty u\left(\frac{\pi(1+\gamma)}{2}-\int_0^\pi\frac{\ln\left(\frac{1+\theta r^\alpha u^{-\alpha}}{1+\theta r^\alpha\ell(u,\varphi)}\right)}{\theta r^\alpha\left(u^{-\alpha}-\ell(u,\varphi)\right)}-\frac{\gamma-1}{2(1+\theta r^\alpha u^{-\alpha})(1+\theta r^\alpha\ell(u,\varphi))}d\varphi\right)du \tag{30}$$

where, $\ell(u,\varphi)=\left(u^2+r^2+2ru\cos\varphi\right)^{-\frac{\alpha}{2}}$

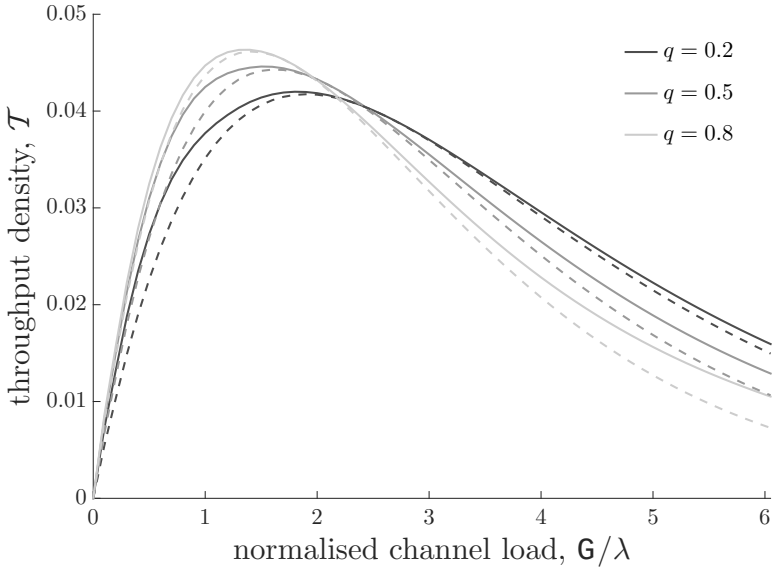

Fig. 9: Throughput density vs normalised channel load G/λ. Solid lines report the behaviour of a system with all transmissions of the same duration, whereas dashed ones indicate the performance achieved when optimising γ. Different shades of grey indicate distinct values configurations for q.

a sound answer to it we compare the two system configurations, referred to as *homogeneous*- and *heterogeneous*-length in the remainder of this section, under the same channel occupancy conditions. From this standpoint, in fact, while in the former case the load evaluates to $\mathsf{G} = \lambda D$, in the latter, assuming half-duplex data exchanges of duration D_{hd}, we have $\mathsf{G} = \lambda D_{\mathsf{hd}}(1+q(\gamma-1))$. Fixing the traffic intensity λ, for any value of G we then operate the heterogeneous network under the $(D_{\mathsf{hd}}, \gamma)$ pair maximising the throughput density in (20), so to understand what is the utmost improvement that can be aimed for. The outcome of this study is reported in Fig. 9 in terms of $\mathcal{T}$ against the normalised load G/λ,[5] keeping the same reference parameters employed in Section III and assuming perfect self-interference cancellation. Within the plot, dashed lines indicate the behaviour of the homogeneous system, whereas solid ones mark the performance of the optimised heterogeneous configuration. Moreover, three sets of curves are reported in different shades of grey, referring to distinct fractions of full-duplex clusters present in the network.

The figure confirms the intuition that operating a hybrid system enforcing a common duration

[5]The normalised load G/λ maps to the packet duration D in homogeneous-length networks, so that the x-axis in the plot is conveniently equivalent to the ones characterising figures discussed in the first part of the paper.

for all communications is not optimal when a completely asynchronous medium access policy is employed. As expected, an heterogeneous setup is especially beneficial when the network is either experiencing low loads or facing congestion. In the former situation, in fact, throughput can be boosted by granting longer data exchanges to bidirectional links while shortening the less profitable half-duplex clusters. Conversely, when high loads are experienced, a reduction in the duration of full-duplex communications in favour of uni-directional ones maps into a lower level of aggregate interference and thus induces a more gentle degradation of the performance. As a result, the additional degree of freedom granted to the system is capable of triggering throughput gains in the order of 15-20% for a broad range of q. On the other hand, such an improvement comes at the cost of a potential unfairness among users, possibly constraining some of them to access the medium only for short information exchanges.

From this standpoint it is thus also insightful to consider the complementary scenario of an existing network characterised by a population of half-duplex clusters transmitting packets of D_{hd} seconds, and investigate how to tune the length of data transfers for advanced full-duplex capable nodes that are progressively introduced into the system. More formally, we are interested in determining the duration ratio γ^* maximising the aggregate throughput density for a certain penetration level q. The solution can be found via numerical optimisation of (20), and is shown in Fig. 10, where distinct lines indicate different configurations in terms of the half-duplex packet length. For large values of D_{hd}, the reference network is already operating with a medium to heavily congested channel, and new full-duplex links shall enjoy much shorter communications not to increase too much the overall interference, regardless of q. On the other hand, when smaller data units are employed by half-duplex pairs (e.g., $D_{\mathsf{hd}} \leq 1$), a notable fraction of the clusters can be upgraded to bidirectional mode and granted channel access for longer fraction of time ($\gamma^* > 1$) bringing an improvement to the system throughput. In this perspective, the developed framework offers then useful tools to evaluate whether it is worth to undergo the cost of deploying full-duplex terminals given the working conditions of an existing topology, taking into account the traffic profiles and applications such new nodes shall be able to sustain.

V. A Comparison with Slotted Schemes

We finally conclude our study by investigating the performance gap between the asynchronous network under consideration and a slotted counterpart of its. The rationale triggering such a

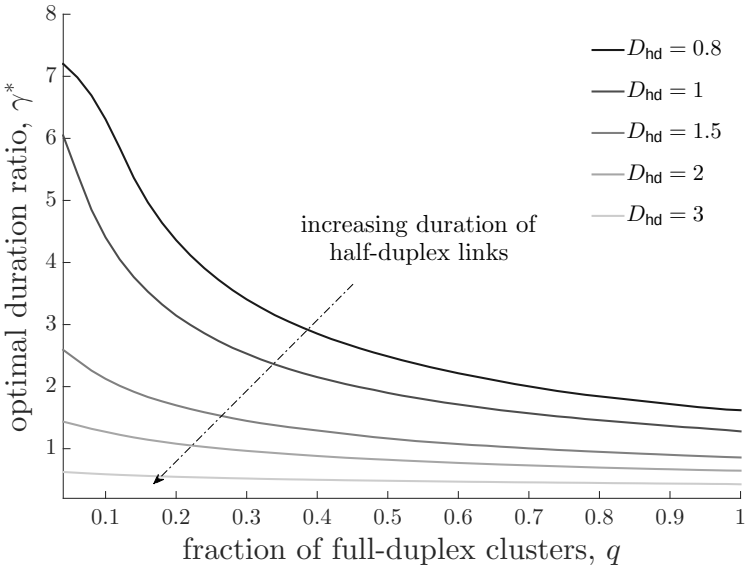

Fig. 10: Ratio of full-duplex to half-duplex transmission duration maximising throughput as a function of q. Different shades of grey report the behaviour for distinct durations D_{hd} of the half-duplex links.

discussion is twofold. On the one hand, the tradeoff between the throughput loss undergone by systems that do not implement any form of coordination among terminals and their intrinsic simplicity is often a basic driver for protocol design and implementation choices and, as such, has been tackled starting from the seminal works of Abramson on Aloha [26]. From this viewpoint, while recent results based on stochastic geometry [23] have provided interesting insights for large and distributed networks, no characterisation is available yet for systems that resort to full-duplex communications. Secondly, the study will allow us to understand the impact of the additional degree of freedom in terms of different packet lengths for half- and full-duplex clusters available in unslotted systems and to clarify whether it can help in reducing the performance degradation with respect to synchronous ones. Throughout our discussion, we will refer to the elegant analysis of slotted full-duplex networks offered in [19], and point the interested reader to it for further details. Instead, we focus in the following on the key results needed for our comparison, and highlight the main conceptual differences with respect to the framework introduced in Section II. In the synchronous scenario, the topology is still composed of pairs of nodes that independently decide whether to establish a bidirectional or a half-duplex link with probability q and $1-q$, respectively. Time is divided in slots of equal duration, and each data exchange in the system

can be performed only within the boundaries of – and fill completely – one such time unit. This element of coordination allows for some major analytical simplifications. Firstly, it decouples the time and spatial components of medium access, so that the network can be effectively described by means of a PPP over $\mathbb{R}^2$ of intensity λ_s [cluster/m^2], with each node pair independently deciding whether to access a slot for an information transfer with probability p. Secondly, the shared time-frame results in a constant level of interference perceived at a receiver for the whole duration of an incoming packet, allowing to overlook the averaging procedures tackled in our work. To ensure a fair comparison, decoding is described via a threshold model for the slotted system as well, and all networking parameters are unchanged with respect to the presented framework. Lastly, we are still interested in evaluating the behaviour of the system as a function of the load, which we defined as the fraction of time the channel is occupied on average. When synchronous access is considered, the dependency of this parameter on the length of transmissions is clearly lost, leading to $\mathsf{G} = p\lambda_s$. Under these modelling assumptions, the system throughput density can be eventually expressed as

$$\mathcal{T}_s = W\mathsf{G}\big(1+q(2\beta-1)\big)\cdot\exp\Big(-\mathsf{G}\big((1-q)\Omega_{\mathsf{hd},s}+q\Omega_{\mathsf{fd},s}\big)\Big) \tag{31}$$

where

$$\Omega_{\mathsf{hd},s} = \pi r^2\theta^{\frac{2}{\alpha}}\Gamma\left(1+\frac{2}{\alpha}\right)\Gamma\left(1-\frac{2}{\alpha}\right),$$
$$\Omega_{\mathsf{fd},s} = \int_0^\infty u\Big(\pi-\frac{1}{1+\theta r^\alpha u^{-\alpha}}\int_0^\pi\frac{1}{1+\theta r^\alpha \ell(u,\varphi)}d\varphi\Big)du$$

and $\ell(u,\varphi)$ is defined in (30).

Leaning on this result, we base our discussion on the performance metric Ξ, defined as the ratio of the throughput of a completely asynchronous configuration to the one of its synchronous counterpart operated at the same channel load G, with equal parameters and fraction of full-duplex clusters. Let us initially assume for the unslotted network all data transmissions to be of the same duration. In this case, a direct comparison of the throughput expressions in (15) and (31) shows how imperfect self-interference cancellation besets the two scenarios in the same way, so that Ξ is in fact independent of β and captures the intrinsic differences between the two access policies beyond specific implementation aspects. The behaviour of the throughput ratio is reported in more details in Fig. 11 as a function of G and of the penetration level q of full-duplex pairs, highlighting how the performance gap widens when the network faces larger channel loads, and

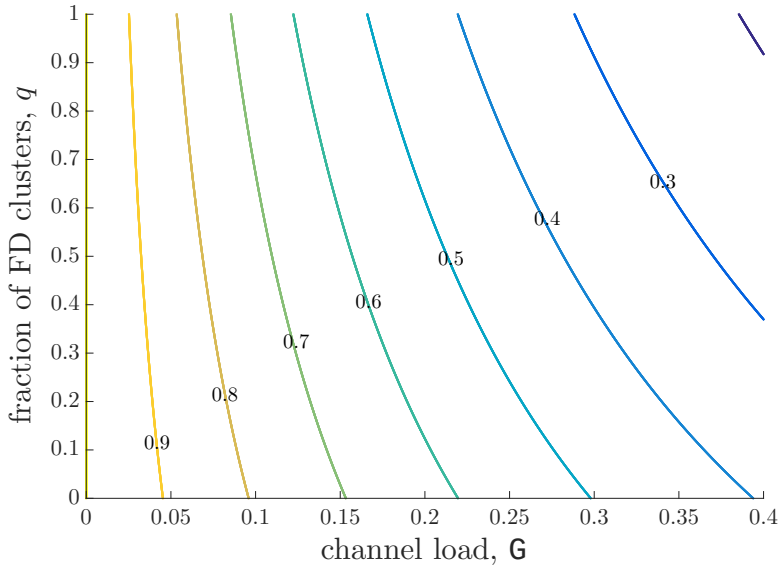

Fig. 11: Ratio Ξ of the throughput density of an unslotted system over a slotted one as a function of the fraction of full-duplex clusters in the network and the channel load. All transmissions in the asynchronous system are of common duration.

confirming the intuition that an increase of aggregate interference is more detrimental in a fully uncoordinated scenario.[6] The same rationale buttresses the similar yet less pronounced trend that can be spotted when more full-duplex transmissions are triggered.

In this perspective, additional insights are offered by Fig. 12, which reports Ξ against q for three different load configurations. Let us first focus on the solid lines, representative of the behaviour of an asynchronous system with common duration for all transmissions, and consider in particular the values for $q = 0$. Such points indicate the performance loss brought by the lack of a slotted time-frame in a traditional completely half-duplex network. Remarkably, when light loads are tackled, synchronism among nodes throughout the network only triggers a 10% gain, making unslotted access particularly attractive in view of its simplicity. Conversely, under strong congestion (e.g., $\mathsf{G} = 0.35$), the performance of an asynchronous MAC plummets to less than half of its slotted competitor. The plot also sheds light on the impact of the additional interference brought by full-duplex connections. It is interesting to observe in fact that, while spatial reuse is

[6]For the sake of comparison, with the traffic density under consideration for the asynchronous case ($\lambda = 0.05$), a channel load $\mathsf{G} = 0.2$ in Fig 11 corresponds to a packet duration $D = 4$ in the plots of Section III (e.g., Fig. 3).

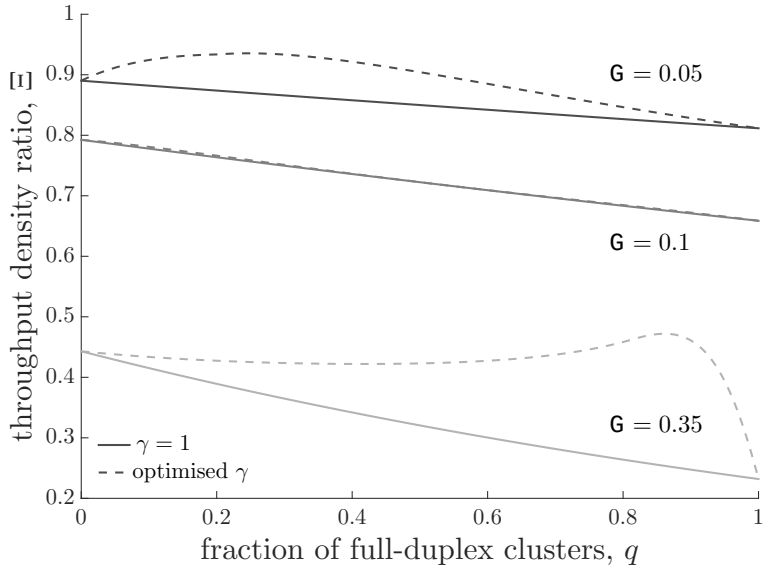

Fig. 12: Ratio Ξ of the throughput density of an unslotted system over a slotted one vs q. Solid lines report the ratio when the asynchronous system is operated with all transmissions of the same duration, whereas dashed ones consider optimal values of γ. Different shades of grey indicate distinct channel loads.

better taken advantage of in slotted systems, the throughput loss undergone in the asynchronous case when increasing q is rather contained, especially for low-to-intermediate load. Along this line of reasoning, it is then relevant to understand whether the gap may be further reduced by leveraging the additional degree of freedom of different transmission durations available in unslotted settings. The question is tackled once more in Fig. 12, where dashed lines report, for any value of q, the performance degradation Ξ undergone by an heterogeneous asynchronous setting whose parameter pair (γ, D) has been configured so as to optimise the throughput in (20). It is apparent how a smarter subdivision of resources in terms of channel occupation time among half- and full-duplex links can partly counterbalance the inefficiency induced by uncoordinated transmissions. Such a result becomes especially remarkable since the benefits are attainable in operating regions of practical interest. For example, if we recall that the traffic intensity of the asynchronous network has been set to $\lambda = 0.05$ throughout our discussion, we can infer that the dashed curve for $\mathsf{G} = 0.05$ in Fig. 12 describes the behaviour of the system for a normalised channel load $\mathsf{G}/\lambda = 1$. This value, in turn, is shown in Fig. 9 to offer a throughput density close to its peak and is thus representative of a working point typically targeted for efficient network

operations.

Beyond numerical results, however, the analytical comparison of slotted and unslotted full-duplex systems enabled by the developed framework shall be seen as a tool towards an educated choice on whether to strive for synchronism or not when designing a system, as it offers insights on some of the key involved performance tradeoffs.

VI. Conclusions

This paper introduced a stochastic geometry framework to capture the performance of an asynchronous Aloha network where part of the nodes operate in full-duplex mode. Closed form expressions have been presented for the success probability and the system throughput, identifying the key tradeoffs in the system. In particular, three operating regions have been identified, showing how for short enough packets as many communications as possible shall be performed in full-duplex mode, while for packets longer than a certain threshold solely relying on half-duplex is convenient. Under the assumption of complete self-interference cancellation, the maximum throughput gain achievable over a purely half-duplex system has been proven to be independent of the distance between source and destination of a link. Bringing imperfect cancellation into the picture, instead, the distance between two communicating nodes becomes a critical parameter, with full-duplex paying off only over short links. An optimisation approach leveraging different link durations for bidirectional and unidirectional data exchanges was introduced to improve network performance and, finally, a comparison with the slotted case studied in [19] was discussed, clarifying the effectiveness cost undergone for not synchronising medium access among devices. In all settings, the role of very accurate self-interference cancellation schemes has been prompted as a necessary condition for full-duplex to be convenient in broad and uncoordinated networking scenarios.

Appendix A
Prof of Theorem 1

We aim to show that $\Omega_{\mathsf{fd}}(r,\theta,\alpha)/\Omega_{\mathsf{hd}}(r,\theta,\alpha)$ does not depend on the distance r between two nodes in a cluster. Recalling from (8) that the denominator can be written in the form $\Omega_{\mathsf{hd}}(r,\theta,\alpha) = k(\theta,\alpha)r^2$, $k \in \mathbb{R}$, the proposition is proven as soon as the numerator exhibits a quadratic dependence on r as well. As a first step, we observe that the definition of Ω_{fd} in (13)

leverages symmetry to compute the spatial average over the cluster center considering a node $\mathbf{u}$ moving along the x axis, i.e., $\mathbf{u} = u e^{j\xi}$, $\xi = 0$. Leaning on the expression $\mathbf{w} = r e^{j\varphi}$ and on the topology of Fig. 1, we can thus reformulate (13) as $\Omega_{\mathsf{fd}} = \int_0^\infty \pi u\, g(u)\, du$, where

$$g(u) = \int_0^\pi 1 - \frac{\ln\big(1+sL(\mathbf{u})\big) - \ln\big(1+sL(\mathbf{u}+\mathbf{w})\big)}{s\big(L(\mathbf{u}) - L(\mathbf{u}+\mathbf{w})\big)}\, d\varphi$$

and $s = \theta r^\alpha$. For a given $\mathbf{u}$ on the x-axis, the integral solely depends on the path loss function $L(\cdot)$ computed at the companion node in the cluster, which in turn is maximised for $\varphi = \pi$, i.e., when $\mathbf{w} = \mathbf{w}' = -r$. Hence, we obtain

$$g(u) \overset{(a)}{\leq} 1 - \frac{\ln\left(\frac{1+su^{-\alpha}}{1+s(u-r)^{-\alpha}}\right)}{s\left(u^{-\alpha} - (u-r)^{-\alpha}\right)} \overset{(b)}{\leq} 1 - \frac{1}{s\,u^{-\alpha}} \tag{32}$$

Here, the first inequality stems from the observation that, for any $\varphi \in [0, \pi]$ it holds

$$L(\mathbf{u}) - L(\mathbf{w}) \leq L(\mathbf{u}) - L(\mathbf{w}')$$
$$\ln\left(\tfrac{1+sL(\mathbf{u})}{1+sL(\mathbf{u}+\mathbf{w})}\right) \geq \ln\left(\tfrac{1+sL(\mathbf{u})}{1+sL(\mathbf{u}+\mathbf{w}')}\right)$$

Conversely, inequality (b) follows by applying to the logarithmic numerator the well-known relation $\ln(x) \geq 1 - 1/x$, $x \in \mathbb{R}$ and by carrying out simple manipulations on the obtained expression. Plugging the bound (32) into the definition of Ω_{fd}, and evaluating the integral over u, we eventually get

$$\Omega_{\mathsf{fd}} \leq r^2\big(\pi\theta^{\frac{2}{\alpha}}\,\Gamma(1+2/\alpha)\,\Gamma(1-2/\alpha)\,\alpha\big) \tag{33}$$

To complement this result, let us focus on the two cases of a solely half-duplex and a solely full-duplex network with ideal self-interference cancellation, corresponding to $q = 0$ and $q = 1$, respectively. Assuming the same set of parameters for the two scenarios, particularly in terms of density λ and link duration D, $p_s^{(\mathsf{hd})} \geq p_s^{(\mathsf{fd})}$ clearly holds, as the full-duplex system undergoes on average a larger level of interference due to the increased spatial reuse. Recalling (4)-(5) and the expressions of the Laplace transforms in (7)-(8), (12), we then get $\exp(-4\lambda\Omega_{\mathsf{hd}}) \geq \exp(-4\lambda\Omega_{\mathsf{fd}})$, leading to

$$\Omega_{\mathsf{fd}} \geq r^2\left(\pi\theta^{\frac{2}{\alpha}}\,\Gamma(1+2/\alpha)\,\Gamma(1-2/\alpha)\,\frac{\alpha}{2(\alpha+2)}\right) \tag{34}$$

Combining (33) and (34), the real-valued analytical function $\Omega_{\mathsf{fd}}(r, \theta, \alpha)$ is lower- and upper-bounded for any $r \in \mathbb{R}$ by curves in the form Ar^2 and Br^2, with A and B real constants. The statement under proof then readily follows from elementary applications of analytical geometry [27]. ■

REFERENCES

[1] M. Duarte and A. Sabharwal, "Full-Duplex Wireless Communications Using Off-The-Shelf Radios: Feasibility and First Results," in *Proc. Asilomar*, Pacific Grove (CA), US, Nov. 2010.

[2] M. Jain, J. Choi, T. Kim, D. Bharadia, S. Seth, K. Srinivasan, P. Levis, S. Katti, and P. Sinha, "Practical, Real-Time, Full Duplex Wireless," in *Proc. ACM MobiCom*, Las Vegas (NV), US, Sep. 2011.

[3] J. I. Choi, M. Jain, K. Srinivasan, P. Levis, and S. Katti, "Achieving Single Channel, Full Duplex Wireless Communication," in *Proc. ACM MobiCom*, Chicago (IL), US, Sep. 2010.

[4] D. Bharadia, E. McMilin, and S. Katti, "Full Duplex Radios," in *Proc. ACM SIGCOMM*, Hong Kong, China, Aug. 2013.

[5] M. Duarte, A. Sabharwal, V. Aggarwal, R. Ramakrishnan, C. Rice, and N. Shankaranarayanan, "Design and Characterization of a Full-Duplex Multiantenna System for WiFi Networks," *IEEE Trans. on Vehicular Technology*, vol. 63, no. 3, pp. 1160–1177, Mar. 2014.

[6] S. Hong, J. Brand, J. Choi, M. Jain, J. Mehlman, S. Katti, and P. Levis, "Applications of Self-Interference Cancellation in 5G and Beyond," *IEEE Communications Magazine*, vol. 52, no. 2, pp. 114–121, Feb. 2014.

[7] A. Sabharwal, P. Schniter, D. Guo, D. W. Bliss, S. Rangarajan, and R. Wichman, "In-Band Full-Duplex Wireless: Challenges and Opportunities," *IEEE Journal on Selected Areas in Communications*, vol. 32, no. 9, pp. 1637–1652, Sep. 2014.

[8] G. Liu, R. Yu, H. Ji, V. Leung, and X. Li, "In-Band Full-Duplex Relyaing: A Survey, Research Issues and Challenges," *IEEE Communications Survey and Tutorials*, vol. 17, no. 2, pp. 500–524, 2015.

[9] Z. Tong and M. Haenggi, "A Throughput-Optimum Adaptive ALOHA MAC Scheme for Full-Duplex Wireless Networks," in *Proc. IEEE GlobeCom*, San Diego (CA), US, Dec. 2015.

[10] N. Singh, D. Gunawardena, A. Proutiere, B. Radunovic, H. Balan, and P. Key, "Efficient and Fair MAC for Wireless Networks with Self-Interference Cancellation," in *Proc. IEEE WiOpt*, Princenton (NJ), US, May 2011.

[11] K. Thilina, H. Tabassum, E. Hossain, and D. I. Kim, "Medium Access Control Design for Full Duplex Wireless Systems: Challenges and Approaches," *IEEE Communications Magazine*, vol. 53, no. 5, pp. 112–120, May 2015.

[12] W. Choi, H. Lim, and A. Sabharwal, "Power-Controlled Medium Access Control Protocol for Full-Duplex WiFi Networks," *IEEE Trans. on Wireless Communications*, vol. 14, no. 7, pp. 3601–3613, Jul. 2015.

[13] V. Cadambe and S. Jafar, "Degrees of Freedom of Wireless Networks With Relays, Feedback, Cooperation, and Full Duplex Operation," *IEEE Trans. on Information Theory*, vol. 55, no. 5, pp. 2334–2344, May 2009.

[14] S. Barghi, A. Khojastepour, K. Sundaresan, and S. Rangarajan, "Characterizing the Throughput Gain of Single Cell MIMO Wireless Systems with Full Duplex Radios," in *Proc. IEEE WiOpt*, Paderborn, Germany, May 2012.

[15] B. Day, A. Margetts, D. Bliss, and P. Schniter, "Full-Duplex MIMO Relaying: Achievable Rates Under Limited Dynamic Range," *IEEE Journal on Selected Areas in Communications*, vol. 30, no. 8, pp. 1541–1553, Sep. 2012.

[16] A. Sahai, S. Diggavi, and A. Sabharwal, "On Degrees-of-Freedom of Full-Duplex Uplink/Downlink Channel," in *Proc. IEEE Information Theory Workshop*, Seville, Spain, Sep. 2013.

[17] O. Simeone, E. Erkip, and S. Shamai, "Full-Duplex Cloud Radio Access Networks: An Information-Theoretic Viewpoint," *IEEE Wireless Communications Letters*, vol. 3, no. 4, pp. 413–416, 2014.

[18] X. Xie and X. Zhang, "Does Full-Duplex Double the Capacity of Wireless Networks?" in *Proc. IEEE INFOCOM*, Toronto, CA, Apr. 2014.

[19] Z. Tong and M. Haenggi, "Throughput Analysis for Full-Duplex Wireless Networks with Imperfect Self-interference Cancellation," 2015. [Online]. Available: http://arxiv.org/abs/1502.07404

[20] P. Gupta and P. Kumar, "The Capacity of Wireless Networks," *IEEE Trans. on Information Theory*, vol. 46, pp. 388–404, Mar 2000.

[21] W. Cheng, X. Zhang, and H. Zhang, "Full-Duplex Spectrum-Sensing and MAC Protocol for Multichannel Nontime-Slotted Cognitive Radio Networks," *IEEE Journal on Selected Areas in Communications*, vol. 33, no. 5, pp. 820–831, May 2015.

[22] A. Gupta and R. Kumar, "A Survey of 5G Network: Architecture and Emerging Technologies," *IEEE Access*, vol. 3, pp. 1206–1232, 2015.

[23] B. Błaszczyszyn and P. Muehlethaler, "Stochastic Analysis of Non-Slotted Aloha in Wireless Ad Hoc Networks," in *Proc. IEEE INFOCOM*, San Diego (CA), US, Mar. 2010.

[24] M. Haenggi, *Stochastic Geometry for Wireless Networks*. Cambridge University Press, 2012.

[25] A. Zanella and M. Zorzi, "Theoretical Analysis of the Capture Probability in Wireless Systems with Multiple Packet Reception Capabilities," *IEEE Trans. on Communications*, vol. 60, no. 4, pp. 1058–1071, Apr. 2012.

[26] N. Abramson, "The Throughput of Packet Broadcasting Channels," *IEEE Trans. on Communications*, vol. 25, no. 1, pp. 117–128, Jan. 1977.

[27] H. Flanders and J. Price, *Elementary Functions and Analytical Geometry*. Academic Press, 1973.